



# HHS Public Access

Author manuscript

*Integr Biol (Camb)*. Author manuscript; available in PMC 2020 January 06.

Published in final edited form as:

*Integr Biol (Camb)*. 2013 January ; 5(1): 29–42. doi:10.1039/c2ib20047c.

## Targeted nanoparticles in imaging: paving the way for personalized medicine in the battle against cancer

Soo J. Shin<sup>#1,2</sup>, Jaymes R. Beech<sup>#1,2</sup>, Kimberly A. Kelly<sup>1,2,†</sup>

<sup>1</sup>Department of Biomedical Engineering, University of Virginia School of Engineering and Applied Sciences; Charlottesville, Virginia.

<sup>2</sup>Robert M. Berne Cardiovascular Research Center, University of Virginia School of Medicine; Charlottesville, Virginia.

# These authors contributed equally to this work.

### Abstract

The way we view cancer has advanced greatly in the past few decades from simplistic approaches to finely honed systems. This transition has been made possible because of advancements on two fronts: the first is the rapidly expanding knowledge base of the mechanisms and characteristics of cancer; the second is innovation in imaging agent design. Rapid advancements in imaging and therapeutic agents are being made through the evolution from one-dimensional molecules to multi-functional nanoparticles. Powerful new agents that have high specificity and minimal toxicity are being developed for *in vivo* imaging. Here we detail the unique characteristics of cancer that allow differentiation from normal tissue and how they are exploited in nanoparticle imaging development. Firstly, genetic alterations, either endogenous or induced through gene therapy, is one such class of characteristics. Proteomic differences such as overexpressed surface receptors is another targetable feature used for enhanced nanoparticle retention. Increased need for nutrients and specific growth signals to sustain proliferation and angiogenesis are further examples of how cancer can be targeted. Lastly, migration and invasion through a unique microenvironment are two additional traits that are exploitable, due to differences in metalloproteinase concentrations and other factors. These differences are guiding current nanoparticle design to better target, image and treat cancer.

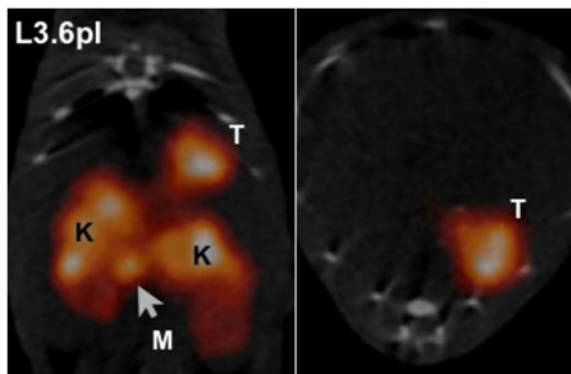
### Graphical Abstract

---

<sup>†</sup>**Corresponding Author:** Kimberly A. Kelly, Department of Biomedical Engineering, University of Virginia, PO Box 800759, Health System, Charlottesville, VA 22908, Phone: 434-243-9352, Fax: 434-982-3870, kak3x@virginia.edu.

Disclosure of Potential Conflicts of Interest

The authors declare no potential conflicts of interest.



This review discusses the unique characteristics of cancer that allow for nanoparticle imaging *in vivo*.

---

## § 1. Introduction

The past few decades have yielded an enormous amount of information on cancer, resulting in tremendous progress in the development of cancer therapies as well as revealing the complexity of the disease. The preponderance of data generated has been obtained in isolation – rarely taking into account how tumors and the environment interact. Because, it is now well established that the tumor and its microenvironment demonstrate considerable cross-talk, influencing signaling cascades as well as aggressiveness, it is important to understand the complex interactions in order to effectively treat cancer.

The current techniques used to detect and assess tumor cells and the microenvironment are limited, often invasive, and destructive. Cell culture experiments have contributed vastly to our knowledge of cancer; however, *in vitro* experiments do not take into account the microenvironment and the complex milieu that profoundly influence the tumor cells. In the case of a biopsy, only a limited section of the tumor is examined, giving the researcher a snapshot of what is happening but not the whole picture. Alternatively, tissue extraction can yield information on the whole tumor, but makes temporal studies difficult. *In vivo* imaging on the other hand can provide information on the tumor in context and its relationship to the body, while being non-invasive and providing the possibility of monitoring temporal progression.

Nanoparticle technology has emerged as a way to develop highly specific *in vivo* imaging agents that can target cancer specific molecules, structures such as vessels, and other components of the tumor microenvironment. Nanoparticles have several advantages as imaging agents as they have 1) large carrying capacities, which can be used to increase the sensitivity of modalities such as high-resolution MR, 2) can be used with multiple imaging modalities, first enable non-invasive imaging then intraoperative imaging to ensure complete tumor removal and cancer free margins, and 3) can be used as theragnostics to allow monitoring of drug to the tumor site.

In this review, we highlight the use of nanoparticles to study each of the tumor compartments *in vivo* as they are responding to signals from the other compartments and the

body. The targetable characteristics of a tumor and its environment used here include: genetic mutations and expression patterns, protein misregulations, uncontrolled proliferation, increased angiogenesis, migration and invasion, and an abnormal microenvironment. By exploiting these characteristics, nanoparticle-mediated imaging has the potential to increase the pace of preclinical research, reshape the way we diagnose and monitor tumors as well as treat cancer.

## § 2.1. Nanoparticles targeting genetic mutations and expression in cancer

One of the most well known characteristics and mechanisms of tumorigenesis is genetic alterations. This may be mutations in the genome, as with p53 or RAS, or misregulation of expression of signaling proteins, such as epidermal growth factor receptor (EGFR). Methods of exploiting these variations have been attempted for the diagnosis and treatment of cancer. Traditionally, the way to measure DNA and mRNA expression was *in situ* hybridization (ISH), which requires fixed samples, limiting its use to histology. However, new methods have recently emerged to monitor mRNA expression *in vitro*, *in situ*, and *in vivo*.

Molecular beacons (MB) were developed in 1996 and have since proven very efficient and successful at detecting real time mRNA levels *in vitro*<sup>1</sup>. Their design utilizes a looped oligonucleotide with a fluorophore to create fluorescence resonance energy transfer (FRET). Through this technique, a detectable signal is achieved only through perfect base pairing of the probe to its target as single nucleotide mismatch will not activate the probe<sup>1</sup>. One of the best examples of MBs in cancer has been their use in detecting the mRNA levels for survivin, an anti-apoptotic protein that is overexpressed in many cancers<sup>2</sup>. Peng *et al.* developed a MB to target survivin mRNA and was able to quantitatively measure the gene expression in cancer cells. The probe has subsequently been used in the detection of breast, bladder and cervical cancer, often with results within an hour<sup>2, 3, 4</sup>.

Beacons have also been designed to utilize their specificity for single nucleotide polymorphisms (SNPs). Secondary mutations in EGFR in non-small cell lung carcinomas (NSCLC) are a common occurrence in EGFR inhibitor therapy resistance. Kim *et al.* developed a MB to rapidly detect this mutation *in situ*. Their results showed the probe had higher sensitivity than direct sequencing<sup>5</sup>. Although these studies have been done *in vitro* or *in situ*, as the field develops, MBs are being used in more complex nanoparticles and for more applications. Upon MBs binding to their target mRNA, they prevent translation and the conjugate becomes flagged for degradation by RNase H<sup>1</sup>, which opens the possibility of a therapeutic aspect to MBs. Kim *et al.* utilize this feature in a theragnostic nanoparticle that uses one aptamer to target and internalize the probe, then a second aptamer as a beacon to microRNA-221, which is responsible for proliferation in cancer. Upon binding, the MB is fluorescently detectable and its binding partner is degraded, significantly reducing tumor volume<sup>6</sup>. These results show the possibilities of MBs to both diagnose and treat multiple types of cancer.

One of the most limiting aspects to MBs however is their reliance on fluorescence, preventing their use in non-optical applications. Alternatively, radiolabeled antisense oligonucleotides (RASONS) have been used for *in vivo* imaging of tumors. These probes

also utilize the high specificity of base pair matching to mRNA but are designed to have a radiolabel for detection of deeper targets *in vivo*. Sato *et al.* has demonstrated this possibility by using RASONS in a polyamidoamine dendrimer conjugated with biotin and avidin to form a nanoparticle aggregate<sup>7</sup>. Their results showed detectable tumor uptake through scintigraphy but noted the probe would benefit from a more stable form of oligonucleotide. Since stability issues are a major concern with antisense probes when used *in vivo*, several modifications to their molecular backbone have been attempted including the use of phosphodiester, a locked nucleic acid formation, and a phosphoramidate morpholino molecule, each having advantages and disadvantages but all greatly increasing their stability<sup>8</sup>. Additionally, antisense probes have been used in combination with polymer and lipid-based nanoparticles and other means to improve their bioavailability and facilitate their entry into the cell<sup>9, 10, 11</sup>. Despite these improvements, the lack of a distinguishable difference between a bound probe and an unbound probe often results in high background, especially when the target mRNA is not highly expressed. This remains a challenge with this technology and will need to be addressed for RASONS to be an effective mRNA imaging agent.

One of the best applications of gene expression imaging occurs with gene therapies. Including a reporter with the target gene allows for new methods of detection not available with endogenous genes alone. Often, a reporter gene will also have an amplified signal since one mRNA can encode for multiple proteins, and each protein could have an amplifying effect<sup>12</sup>. A simple example of such a system would use green fluorescent protein (GFP) or luciferase as a reporter, which will be expressed with the target gene. Other approaches have been made for use with non-optical systems such as the use of a  $\beta$ -Galactosidase reporter to enzymatically react with a specialized nanoparticle for imaging. The nanoparticle uses a caged paramagnetic ion that is encapsulated by the cleavable substrate galactopyranose preventing the ion's interaction with water molecules, effectively dampening its detectable signal via MRI. When the substrate is cleaved by  $\beta$ -Galactosidase, the ion can interact with water and produce a much stronger MRI signal<sup>13</sup>. Another reporter gene encodes a unique receptor based on a modified transferrin protein. By using monocrystalline iron oxide nanoparticles (MION) coated with a protecting layer of dextran and conjugated to holo-transferrin for targeting, the engineered receptor enhances internalization of the nanoparticle and allows for detection by the increased accumulation in the target cells<sup>14</sup> (Fig. 1).

As the field of imaging gene expression develops, powerful new techniques will prove invaluable for the early diagnosis, monitoring, and treatment of cancer. As a relatively new class of imaging agents, mRNA monitors are still evolving. Several key challenges need to be overcome before they are used effectively in the clinic. Most notably, a bridge needs to be found for the gap between highly sensitive but optically limited beacons and radiolabeled antisense oligonucleotides, which have *in vivo* detectability but also a poor signal to noise ratio. Improvements in these areas will vastly increase the usefulness of RNA probes and therapies especially with the emerging field of theragnostics.

## § 2.2. Nanoparticles targeting protein overexpression, deregulation, and misregulation

As a result of the genetic mutations and misregulations, cancer has a unique proteome providing yet another targeting mechanism for tumor imaging. Serum proteins such as PSA have strong benefits as markers because of their convenience, but these are also rare to find and often yield unreliable results. Additionally, serum markers do not indicate the locations of the tumor. Alternatively, proteins in the tumor cells are a much more reliable and abundant source of biomarkers. Intracellular proteins can serve as great tools with histology, but noninvasive imaging agents usually cannot enter the cytosol of cancer cells, rendering the markers inaccessible. Thus, the majority of imageable proteins are on the cell surface and in the extracellular matrix.

Cell surface proteins have allowed for one of the best methods of targeting cancer for molecular probes and nanoparticles. Detectable proteins can be absent/underexpressed, unnaturally present/overexpressed, or mutated/misregulated. Using these markers allows for several benefits with imaging and treatment, such as direct localization and demarcation of the tumor mass. Additionally, many of these proteins have a function in sustaining the tumor and targeting them can yield insight into the tumor's biology. Often, upon binding of the targeting agent, the protein-nanoparticle complex will internalize, enhancing the agent's imaging or therapeutic efficacy.

Early known markers have often included overexpressed receptors because they reside in the plasma membrane and initiate intracellular signaling for growth, proliferation, and survival. For example, human epidermal growth factor receptor 2 (HER2), EGFR, and vascular endothelial growth factor receptor 2 (VEGFR2) have all shown to be overexpressed in many forms of cancer such as breast, lung and colon. Monoclonal antibodies such as Herceptin, Erbitux or Avastin respectively, are used to target and therapeutically control these proteins with great success but they also provided a means for targeting the tumor for imaging and diagnostic purposes. Recently Rasaneh *et al.* used Trastuzumab, an antibody against HER2, in combination with a dextran-coated iron oxide to make modified magnetic nanoparticles for detection of breast cancer. Their findings showed significant uptake of the nanoparticles in the cancer cells compared to the untargeted nanoparticles. Biodistributions from mouse studies showed a higher density of nanoparticles in the tumor than any of the organs, including the liver<sup>15</sup>.

Because of the large size, cost, and immunogenic properties of antibodies, alternative targeting methods have been used for biomarkers such as receptors. One of the most obvious methods is to use the ligand that is specific for that protein. This has been used successfully with folate receptors, which are overexpressed in most cancers. Folic acid had been conjugated to Technetium-99m Labeled PEGylated Dendrimer Poly(amidoamine) (PAMAM) nanoparticles for detection of cancer via SPECT. By adding the folic acid to target its receptor on cancer, imaging results showed uptake in the cancer mass but not the surrounding tissue<sup>16</sup>.

In addition to receptors, other surface proteins have also been used. Carcinoembryonic antigen (CEA) and epithelial cell adhesion molecule (EpCAM) are some of the most widely used proteins for targeting cancer<sup>17</sup>. Another example, plectin, has been used for the detection of pancreatic cancer in animal models. Plectin is naturally expressed in almost all cell types, but intracellularly. In pancreatic cancer, plectin is localized on the cell surface, accessible to targeting nanoparticles. Kelly *et al.* discovered this phenomenon using a phage display screen to compare normal and cancerous cells. They subsequently developed a peptide that specifically targets the mislocalized plectin<sup>18</sup>. The peptide has since been incorporated into a tetrameric nanoparticle (tPTP) and conjugated to a radiolabel for imaging. Because plectin is expressed in 100% of pancreatic cancer tumors and their subsequent metastases, but not normal pancreas, it has yielded great success as an imaging agent and is entering clinical trials<sup>19</sup> (Fig. 2).

In addition to cancer detection and diagnosis, targeted nanoparticles have also been developed for monitoring response to chemotherapeutic drugs. When cells undergo apoptosis, numerous changes occur to their proteome, DNA becomes destroyed and the plasma membrane becomes “flipped” exposing the inner surface. These changes allow for imaging agents to selectively bind apoptotic cells. For example, Zhao *et al.* used the noninvasive MR contrast agent SPIONs conjugated to C<sub>2</sub> domain of synaptotagmin I<sup>20</sup>, which was shown to bind to the plasma membrane of apoptotic cells<sup>21</sup>. They found that C<sub>2</sub>-SPIONs were relatively non-toxic, and could detect apoptotic cells with high spatial resolution compared to magnetic resonance spectroscopy (MRS) and radionuclide techniques<sup>20</sup>. Annexin-V, which has a high specificity and affinity for phosphatidylserine in apoptotic cells, is another target being explored for imaging apoptosis via iron oxide nanoparticles. Annexin V-targeted crosslinked iron oxide nanoparticles (CLION) were able to identify cell suspensions containing apoptotic cells *in vitro*<sup>22</sup>.

Proteomic differences are one of the most utilized mechanisms for molecularly targeting tumors. They provide a combination of imaging and therapy because many of the discovered targets have a functional roll in tumor biology. Proteomics are being used to classify cancer as well. Screens for markers of sensitivity and resistance to therapies are one of the most promising examples<sup>23</sup>. The results of such studies will help guide treatments and direct the standard of medicine to a more personalize approach. Knowledge of one’s tumor proteome will provide significant insight into the therapies that will be most effective on an individual basis, minimizing unnecessary, toxic treatments resulting in improved patient outlook and quality of life.

### § 2.3. Nanoparticles targeting cancer cell proliferation and metabolism

One of the most fundamental signatures of cancer is its ability to sustain uncontrolled growth. In normal tissue, proliferative and apoptotic signals are tightly regulated to maintain tissue homeostasis and differentiation<sup>24, 25</sup>. However, cancer cells deregulate genes involved in these processes to maintain cell survival<sup>26</sup>. Thus, noninvasive detection of cancer cell proliferation, metabolism, and resistance to apoptosis may be useful clinically for monitoring disease progression and for effectively assessing therapeutic response.

cis-Dichlorodiamminoplatinum (II) (cisplatin), which disrupts the cell division process, has demonstrated activities against a variety of solid tumors. However, the clinical efficacy of cisplatin is limited by its toxic profile<sup>27</sup>. To reduce the toxic effects and enhance circulation time, Li *et al.* designed nanoparticles from methoxy poly(ethylene glycol)-polycaprolactone (mPEG-PCL) with a core-shell structure that encapsulates cisplatin. This copolymer-based nanoparticle demonstrated sustained release of cisplatin and efficacy against BGC823 and H22 tumors in dose and time-dependent manner. They reported that intratumoral delivery of cisplatin-loaded nanoparticles demonstrated delayed tumor growth compared with free cisplatin. The noninvasive imaging with <sup>18</sup>F-fluorodeoxyglucose (<sup>18</sup>F-FDG)-positron emission tomography (<sup>18</sup>F-FDG-PET) combined with computed tomography (CT) for anatomical imaging showed that <sup>18</sup>F-FDG uptake was lower in mice receiving cisplatin-loaded nanoparticles intratumorally (Fig. 3)<sup>28</sup>. This study shows that polymeric nanoparticles with core-shell structures may be useful clinically in future as drug delivery carriers. Although this study did not incorporate an imaging agent together with the drug-delivering nanoparticle, polymeric nanoparticles can simultaneously encapsulate both imaging agents detectable by MRI and drugs for theragnostic applications<sup>29</sup>.

Transferrin is a plasma protein that functions in iron transport<sup>30</sup>. Many studies have demonstrated that transferrin is expressed on proliferating cells and is an essential requirement for cellular proliferation<sup>30, 31, 32</sup>. Therefore, transferrin serves as a good target for imaging proliferating cancer cells. Huang *et al.* demonstrated the use of viral nanoparticle (VNP) that target transferrin. They were able to target cancer cells *in vitro* by covalently conjugating transferrin onto the surface of HK97-based VNPs. To visualize the target, they conjugated VNPs with fluorescein-5-maleimide and showed that the VNPs were internalized and localized to the endolysosomal compartment via confocal microscopy<sup>33</sup>. VNPs can be readily modified to incorporate MRI contrast agents as well because genetic modification or chemical conjugation can easily add new functionalities to VNPs<sup>34</sup>. Liepold *et al.* have shown that gadolinium chelating moieties can be fused to VNP surface to yield high relaxivity, resulting in improved sensitivity in MRI<sup>35</sup>. Furthermore, viruses naturally infect specific host cells and deliver encapsidated nucleic acids with great efficiency<sup>36</sup>. Therefore, VNPs may have potential for clinical applications in cancer therapy.

Telomerase is a DNA polymerase that maintains telomere length and function. It is almost absent in normal cells, but elevated levels of telomerase activity are found in spontaneously immortalized cells, including human cancer cells<sup>26</sup>. It has been shown that telomerase activity is correlated with a resistance to cellular senescence and apoptosis and therefore believed to play a critical role in tumorigenesis<sup>26, 37</sup>. Grimm *et al.* developed a nanosensor that is capable of rapidly screening telomerase activity. This nanosensor system was designed by conjugating oligonucleotides (telomerase synthesized TTAGGG repeats) to amidated cross-linked iron oxide nanoparticles (CLION-NH<sub>2</sub>). In addition to monitoring telomerase activity, they were able to determine the efficacy of different telomerase inhibitors via high-throughput MRI with ultrahigh sensitivities. In this application, magnetic nanoparticles and MRI served as a powerful tool for rapidly detecting telomerase activity<sup>37</sup>.

There are many genes and proteins that are involved in maintaining the pro-proliferative state of cancer cells. For example, folate receptors are overexpressed in various types of

cancers including ovarian, endometrial, breast, and renal cell carcinomas<sup>16</sup> and were shown to play an essential role in cell proliferation and survival<sup>38</sup>. Targeting proliferation allows for the noninvasive detection of aggressive cancer cells. Development of nanoparticles that target biomarkers critical for cancer cell proliferation and apoptosis-evasion will have powerful clinical effects. Not only will these help monitor disease progression and therapeutic response, but also provide insights to which therapies will limit or even reverse tumor growth.

## § 2.4. Nanoparticles targeting tumor vasculature and sustained angiogenesis

Angiogenesis plays a crucial role in normal embryonic vascular development and wound healing, but in cancer, this process is deregulated to allow for growth, invasion, and metastasis of the tumor by providing necessary oxygen and nutrients<sup>39</sup>. Tumor angiogenesis typically involves vessel overgrowth, leaky vasculature, and vessel tortuosity by upregulating angiogenic factors like VEGF and integrin  $\alpha_v\beta_3$ <sup>40</sup>. Without angiogenesis, tumors cannot grow due to lack of oxygen and nutrients<sup>41</sup>. Due to the significant role that angiogenesis has on tumor invasion and metastasis, targeting angiogenesis has become a major therapeutic avenue for cancer treatment. The limited endothelial pore size in the tissue is one of the main biological barriers for nanoparticles. Small molecules can readily diffuse into the tissue through the capillary wall due to their size, but nanoparticles rely on the gap junctions between endothelium to cross the barrier<sup>42</sup>. However, tumor vasculature is primed for passive targeting because nanoparticles can spontaneously extravasate and accumulate in tumors with leaky vasculature by an enhanced permeability and retention (EPR) effect<sup>43</sup>.

In the absence of passive targeting, the most highly studied protein is integrin  $\alpha_v\beta_3$  due to its overexpression in a variety of cancer<sup>39, 44</sup>. Arg-Gly-Asp (RGD) peptide motifs have been known to facilitate binding to integrins on the cell surface and have subsequently been demonstrated to have a strong affinity for integrin  $\alpha_v\beta_3$ <sup>45, 46</sup>. Zhang *et al.* designed integrin  $\alpha_v\beta_3$ -targeted ultrasmall superparamagnetic iron oxide nanoparticles (USPIONs) that are coated with 3-aminopropyltrimethoxysilane (APTMS) and conjugated with cyclic RGD peptides. They showed that RGD-USPIONs resulted in a significantly higher uptake in human umbilical vein endothelial cells (HUVECs) compared to unlabeled USPIONs. Moreover, these nanoparticles were shown to definitively distinguish between tumors with high and low integrin  $\alpha_v\beta_3$  expression levels using a clinical 1.5-T MR scanner<sup>47</sup>. Winter *et al.* used  $\alpha_v\beta_3$ -targeted perfluorocarbon nanoparticles ( $\alpha_v\beta_3$ -PFC) encapsulating fumagillin, which was shown to suppress angiogenesis by inhibiting methionine aminopeptidase 2<sup>48</sup>, to target and image tumor angiogenesis in a rabbit tumor model. They modified the  $\alpha_v\beta_3$ -targeted nanoparticles with ultrahigh payloads of paramagnetic chelates for high resolution imaging and reported that treatment with  $\alpha_v\beta_3$ -PFC-fumagillin resulted in the inhibition VX2 adenocarcinoma development via quantitative MRI<sup>49</sup>. In a more novel approach, Kluza *et al.* used a bimodal system where they functionalized paramagnetic liposomal nanoparticle with two angiogenesis-specific targeting ligands,  $\alpha_v\beta_3$ -targeted RGD and galectin-1-targeted anginex. This synergistic targeting of the two ligands resulted in improved specificity of the liposomal MR contrast agent in a murine tumor model<sup>50</sup>.



The process of angiogenesis is regulated by a variety of stimulating factors including VEGF<sup>51</sup>, fibroblast growth factor (FGF)<sup>52</sup>, and angiopoietin<sup>53</sup>. The VEGF-A gene encodes ligands that are involved in forming new blood vessel during embryonic development, homeostatic survival of endothelial cells, and wound healing<sup>26</sup>. Thus, VEGF-targeted therapeutic strategies have undergone extensive research. In the study by Backer and colleagues, boronated dendrimers containing VEGF<sub>121</sub> successfully targeted VEGF receptors on tumor vasculature. Importantly, these dendrimers were conjugated with near-IR Cy5 dye to allow for near-IR fluorescent imaging of the tumor vasculature<sup>54</sup>. Dendrimers are advantageous due to their biocompatibility, solubility in water, small size with rapid blood and renal clearance, and modification flexibility<sup>29, 55</sup>. Reichardt *et al.* reported that magnetic iron oxide nanoparticles (MIONs) and steady-state MRI enabled an early detection of tumor response to anti-angiogenic therapy with VEGF receptor tyrosinase kinase inhibitors in an animal model of drug-resistant colon carcinoma. They used T2-type MIONs because of their negligible extravasation into the tumor interstitium and therefore allow more precise measurement of vessel volume fraction. In addition, due to the ultralong blood half-life of MION, Reichardt *et al.* were able to perform quantitative analysis of changes in tumor vasculature at very early stage of anti-angiogenic treatment<sup>56</sup>.

In a study by Reddy *et al.*, multifunctional nanoparticles (MNPs) for *in vivo* MRI enhancement and photodynamic therapy (PDT) were used to treat brain cancer. This MNPs targeted tumor vasculature by conjugating with vascular homing peptide, F3. MNPs were also conjugated with the photoactivable agent Photofrin and the contrast agent iron oxide encapsulated by PEG. Reddy *et al.* showed that significant MRI contrast enhancement was achieved in intracranial 9L gliomas upon MNP administration. In addition, treatment with targeted nanoparticles followed by PDT showed a significant improvement in survival in tumor-bearing rats compared to rats that received non-targeted nanoparticles or systemic Photofrin (Fig. 4)<sup>57</sup>.

Although many preclinical studies involving VEGF-targeted nanoparticles have shown promising results, these therapies often failed when entering clinical trials. Although the reason for this is still unclear, Jain argues that a better approach would actually be to normalize vessels, as opposed to inhibiting them, to increase drug delivery efficacy<sup>40</sup>. Because of the complexity of tumor vasculature, again a personalized approach may be needed; methods to image angiogenesis and key markers will be necessary for this to be possible.

## § 2.5. Nanoparticles targeting tissue invasion and metastasis

One of the greatest challenges in cancer is metastasis, the spread of cancer cells from a primary tumor to distant organs<sup>58</sup>. For example, most patients diagnosed with pancreatic cancer present with metastatic disease due to lack of specific symptoms and early detection methods<sup>59</sup>. In addition, surgical resection is seldom a remedy for metastatic cancer, and other treatment options are limited<sup>60</sup>. As a result, tremendous research efforts have been devoted to preventing metastasis.

Nanoparticle design including size and charge is especially important in metastases imaging. Traditional lipid and polymer-based nanoparticles are approximately 100 nm in size<sup>61</sup>. To image metastasis, smaller nanoparticles have an advantage because they can access areas such as lymph nodes and avoid the liver, which is a common site of metastasis. However, if drugs are not encapsulated in nanoparticles with appropriate size, they are prone to renal clearance as well as drug-metabolizing enzymes in the liver before they reach the metastasized tumor. A recent study has shown that the renal excretion threshold is approximately 5.5 nm<sup>62</sup>. Due to this cutoff size, the nanoparticles need to be designed at a smaller size than liposomes, but larger size than small molecules to reduce renal filtration. In addition, drugs must be encapsulated to avoid liver metabolism before being released. This allows for extended blood circulation with higher accumulation in the target and metastatic tissue<sup>63</sup>.

Nanoparticles have been used in clinical studies for detecting lymph node metastases. Preoperative nodal staging has been an important prognostic factor in the treatment of any patient with malignant tumors<sup>64</sup>. However, current techniques used for imaging lymph node metastases are still limited in accuracy because they primarily rely on node size; metastases can often result in non-enlarged lymph nodes or nodal enlargement may not be due to metastases<sup>65</sup>. This limitation has led to the development of lymphotropic nanoparticle enhanced magnetic resonance imaging (LNMRI) as a strategy for nodal evaluation.

Ferumoxtran-10, an USPIO, has been used preoperatively in LNMRI of various cancers including head and neck<sup>66, 67</sup>, urinary bladder cancer<sup>68</sup> and prostate cancer<sup>69</sup>. Deserno *et al.* reported that 10 of 12 normal-sized metastatic lymph nodes were detected with ferumoxtran-10 MRI in urinary bladder cancer patients, which were not detected in precontrast imaging. They also found that ferumoxtran-10 MRI resulted in improved sensitivity (from 76% to 96%) and no significant difference in specificity (from 99% to 95%) compared to precontrast imaging<sup>68</sup>. In prostate cancer patients, Ross *et al.* showed that LNMRI using ferumoxtran-10 was able to detect lymph node metastases in patients that were previously negative for nodal involvement<sup>69</sup>. Stadnik *et al.* used USPIO-MRI in combination with <sup>18</sup>F-FDG-PET for preoperative axillary lymph node staging in breast cancer patients. They found that the combination of USPIO-enhanced MR and FDG-PET achieved 100% sensitivity and specificity<sup>70</sup>.

Several groups have focused on designing nanoparticles that target the matrix metalloproteinases (MMPs), which are involved in tumor invasion and metastasis by degrading extracellular matrix and increasing reactive oxygen species (ROS) activity<sup>26, 71</sup>. ROS contributes to oxidative stress, which contributes to cancer aggression and invasion<sup>71</sup>. Metallofullerenol has been shown to inhibit MMPs and subsequently reduced tumor invasion. Meng *et al.* reported that gadolinium metallofullerenol nanoparticles (f-NPs) targeted MMPs and exhibited anti-metastatic properties in human breast cancer in animal models. Moreover, bioluminescence imaging of f-NPs showed that animals treated with these nanoparticles resulted in significantly less metastasis of the primary breast tumor to the ectopic sites (Fig. 5)<sup>72</sup>. Olson *et al.* designed fluorescent dendrimeric nanoparticles conjugated with activatable cell penetrating peptides (ACPPs) to target and visualize MMPs by fluorescence imaging. In addition, ACPPs were labeled with gadolinium for MRI. They

showed that, compared to free ACPPs, the ACPP conjugated dendrimeric nanoparticles resulted in a much higher uptake in tumors. Since these nanoparticles were labeled with fluorescent molecules, micrometastases as small as 200 $\mu$ m were detectable. This approach has an advantage over single modality therapy because it is translatable to MRI. With relatively high levels of gadolinium accumulating in tumors, this approach could improve T1 contrast in MRI and be useful in MRI-guided clinical staging and intraoperative fluorescence-guided surgery<sup>73</sup>.

Despite adjuvant therapy, most patients die of metastatic cancer. Hence, nanoparticles that enable early detection before tumors metastasize could vastly enhance a patient's therapeutic outcome. The discovery of novel biomarkers involved in cancer cell migration and invasion as well as development of nanoparticles that can effectively prevent further metastasis will greatly improve patient prognosis.

## § 2.6. Nanoparticles targeting tumor microenvironment

To develop effective therapeutic strategies using nanoparticles for target-specific delivery of drugs to tumors, it is important to understand the microenvironment of the tumor. Cancer cells are surrounded by a complex milieu of extracellular matrix (ECM), leaky blood vessels, infiltrating immune cells, and stromal cells. While the normal cellular surroundings prevent malignant cell growth, the tumor surroundings support cell proliferation. Moreover, the tumor microenvironment is characterized by abnormal physiological conditions such as hypoxia and acidic extracellular pH<sup>74</sup> that may induce adaptive changes in both cancer and stromal cells<sup>75</sup>. The tumor microenvironment also creates barriers that prevent therapeutic agents from reaching cancerous cells and thus limits their efficacy<sup>76</sup>.

An important factor in the tumor microenvironment is the ECM, which has a considerable effect on cancer cell proliferation, adhesion, migration, and metastasis<sup>77, 78</sup>. Because proteases like MMPs are involved in degradation of the ECM, targeted imaging of MMP activity has been exploited to monitor tumor cell-ECM interaction<sup>73</sup> (See section §2.5 for examples).

Secreted protein acidic and rich in cysteine (SPARC), an ECM-associated glycoprotein that modulates cell-matrix interactions<sup>79</sup>, has been shown to play a role in various mechanisms including disruption of cell adhesion<sup>80</sup> and ECM remodeling<sup>81</sup>. In addition, high SPARC expression levels correlated with poor prognosis in breast, lung, pancreas, and prostate cancer<sup>82</sup>. Our group recently functionalized biocompatible, fluorescent nanoparticles with an iron oxide core and SPARC-targeted peptide sequence for *in vivo* imaging. Fluorescence-mediated tomography (FMT) revealed that the nanoparticles specifically bound to SPARC in prostate cancer cells both *in vitro* and *in vivo*. Moreover, bone and lung metastases were imaged using SPARC-targeted nanoparticles<sup>83</sup>. This approach provides prognostic information that could be clinically translated for designing personalized treatment strategies.

SPARC has also been shown to play an important role in macrophage infiltration and transmigration<sup>84, 85, 86</sup>, key components of the immune response. A high degree of

macrophage infiltration is associated with a poor prognosis in many cancer types including breast, cervix, and bladder carcinomas<sup>87</sup>. In addition, tumor-associated macrophages (TAMs) were shown to increase tumor growth and metastasis by suppressing the activity of CD8+ T cells<sup>88</sup>. Therefore, TAMs has been considered as novel targets for anti-cancer therapy. One particular approach involves the use of MRI and ferumoxytol, a second generation USPIO in phase II clinical trials, for non-invasive targeting and visualization of TAMs in breast cancer. In this study, Daldrup-Link *et al.* showed that iron oxide nanoparticles were phagocytosed by TAMs but not by tumor cells. In an animal breast cancer model, they were able to detect TAMs via iron oxide nanoparticle-enhanced MRI<sup>89</sup>. Since ferumoxytol is a clinically available nanoparticle, it can be applied for TAM imaging in patients with breast cancer.

Tumors are more acidic when compared to normal tissue<sup>90</sup>. Due to this pH gradient, cancer cells are more likely to accumulate drugs that are weak acids compared to drugs that are basic<sup>91</sup>. Recent cancer treatment strategies have taken advantage of the tumor cell-microenvironment pH gradient. For example, Bae *et al.* designed polymeric micelle drug delivery systems that are designed to release drugs when they encounter the acidic environment in tumors. These lipid-based nanoparticles consist of a polymer shell (PEG) conjugated with a molecular promoter, folate, for enhancing intracellular transport, hydrazone, and an anticancer drug Adriamycin. Because many cancer cells overexpress folate-binding proteins, folate-conjugated micelle nanoparticles would specifically target cancer cells (See § 2.2 for more on folate receptors). The hydrazone bonds are cleaved under acidic conditions, Adriamycin was released in a pH-controlled manner into the tumor microenvironment<sup>92</sup>. Although this study used NMR and flow cytometry to analyze data, the nanoparticles can be easily modified to conjugate imaging agents that are more translatable to clinic. Lim *et al.* took a similar approach by using magnetic nanoparticles and MRI. They used  $\alpha$ -pyrenyl- $\omega$ -carboxyl poly(ethylene glycol) to encapsulate doxorubicin (DOX) and iron oxide nanoparticles that are conjugated with anti-HER2/neu antibody. They demonstrated that these drug-delivering magnetic nanoparticles were pH-responsive and released DOX under low pH conditions. Additionally, these nanoparticles allowed for simultaneous tumor detection and drug delivery, real-time monitoring via MRI *in vivo*, and synergistic therapeutic efficacy between DOX and antibody-mediated suppression of the cell growth signals (Fig. 6)<sup>93</sup>.

Another major characteristic of tumor microenvironment is hypoxia. Hypoxia results from inadequate oxygen supply and abnormal tumor metabolism. In addition, hypoxic microenvironment of tumors often leads to drug resistance, resulting in poor clinical outcome<sup>94, 95</sup>. Because of this, the development of imaging probes for monitoring tumor hypoxia has been of considerable interest for cancer diagnostics and evaluation of therapies. Recently, nitroimidazole and its derivatives have been used to image tumor hypoxia and monitor therapeutic progress<sup>96</sup>. Further, <sup>18</sup>F-fluoromisonidazole (F-MISO) has been used commonly in PET imaging of hypoxia<sup>97</sup>. Polymer-based nanoparticles have also been used in hypoxia imaging in cancer. Napp *et al.* conjugated polystyrene nanoparticles with oxygen-sensitive near-infrared (NIR) emissive palladium mesotetraphenylporphyrin to image tumor hypoxia. The nanoparticle surface was functionalized with PEG and Herceptin to specifically target HER2/neu overexpressing cancer cells. They demonstrated that the use of

oxygen-sensitive dye allowed for imaging tumor hypoxia and the nanoparticles were efficiently delivered both *in vitro* and *in vivo*<sup>98</sup>.

These studies highlight the critical role the microenvironment plays in tumor progression, and thus cannot be dissociated from cancer cells. Nanoparticles that target tumors and their surroundings may provide new insights on how we can treat the disease holistically, rather than focusing on cancer cells only.

### § 3. Conclusion

In recent years, a variety of nanoparticles have been developed exploiting the targetable characteristics of cancer, allowing for non-invasive imaging of tumors. Nanoparticles often utilize only one of the characteristics of cancer and to see their full potential, nanoparticles of the future should attack several of cancer's specific signatures. For example, cancer's unique proteome provides a mechanism for nanoparticles to deliver payloads with high specificity and enhancing efficacy while minimizing toxicity. The abnormal microenvironment of cancer can also be exploited to further attract or activate the nanoparticles, either releasing a therapeutic compound or amplifying the signal from an imaging agent. Additionally, the active proliferation of tumors provides a target that can be monitored to shed light on the tumors status. The patient's specific tumor profile, often classified by the genome and proteome, will help guide the specific moieties used to deliver therapeutic payloads. Because of their multifunctionality and customizability, nanoparticles will play a large role in the development of the personalized medicine necessary to combat the complexity and uniqueness of a patient's cancer.

### Acknowledgments

**Grant support:** This material is based upon work supported by the National Institute of Health under Grant No. R01 CA137071, R01 EB010023, 2T32GM8715-11, and the National Science Foundation Graduate Research Fellowship under Grant No. DGE-0809128.

### References

1. Tyagi S, Kramer FR, Molecular beacons: probes that fluoresce upon hybridization. *Nat Biotechnol* 1996, 14 303–8, DOI: 10.1038/nbt0396-303. [PubMed: 9630890]
2. Peng XH, Cao ZH, Xia JT, Carlson GW, Lewis MM, Wood WC, Yang L, Real-time detection of gene expression in cancer cells using molecular beacon imaging: new strategies for cancer research. *Cancer Res* 2005, 65 1909–1917. [PubMed: 15753390]
3. Xue Y, An R, Zhang D, Zhao J, Wang X, Yang L, He D, Detection of survivin expression in cervical cancer cells using molecular beacon imaging: new strategy for the diagnosis of cervical cancer. *Eur. J. Obstet. Gynecol. Reprod. Biol* 2011, 159 204–208. [PubMed: 21752529]
4. Zhao J, Wang ZQ, Wang XY, Yang XJ, He D, Preliminary study of diagnostic utility of molecular beacons in bladder cancer. *Urology* 2010, 76 512 e8–13.
5. Oh YH, Kim Y, Kim YP, Seo SW, Mitsudomi T, Ahn MJ, Park K, Kim HS, Rapid detection of the epidermal growth factor receptor mutation in non-small-cell lung cancer for analysis of acquired resistance using molecular beacons. *J Mol Diagn* 2010, 12 644–52, DOI: S1525-1578(10)60109-2 [pii] 10.2353/jmoldx.2010.090208. [PubMed: 20805561]
6. Kim JK, Choi KJ, Lee M, Jo MH, Kim S, Molecular imaging of a cancer-targeting theragnostics probe using a nucleolin aptamer- and microRNA-221 molecular beacon-conjugated nanoparticle. *Biomaterials*. 2012, 33 207–2017. [PubMed: 21944470]

7. Sato N, Kobayashi H, Saga T, Nakamoto Y, Ishimori T, Togashi K, Fujibayashi Y, Konishi J, Brechbiel MW, Tumor targeting and imaging of intraperitoneal tumors by use of antisense oligo-DNA complexed with dendrimers and/or avidin in mice. *Clin Cancer Res* 2001, 7 3606–12. [PubMed: 11705883]
8. Lendvai G, Estrada S, Bergstrom M, Radiolabelled oligonucleotides for imaging of gene expression with PET. *Curr Med Chem* 2009, 16 4445–61, DOI: CMC - AbsEpub - 060 [pii]. [PubMed: 19835563]
9. Elazar V, Adwan H, Rohekar K, Zepp M, Lifshitz-Shovali R, Berger MR, Golomb G, Biodistribution of antisense nanoparticles in mammary carcinoma rat model. *Drug Deliv* 2010, 17 408–18, DOI: 10.3109/10717541003777225. [PubMed: 20429847]
10. Fu P, Shen B, Zhao C, Tian G, Molecular imaging of MDM2 messenger RNA with 99mTc-labeled antisense oligonucleotides in experimental human breast cancer xenografts. *J Nucl Med* 2010, 51 1805–12, DOI: jnumed.110.077982 [pii] 10.2967/jnumed.110.077982. [PubMed: 20956468]
11. Koh CG, Zhang X, Liu S, Golan S, Yu B, Yang X, Guan J, Jin Y, Talmon Y, Muthusamy N, Chan KK, Byrd JC, Lee RJ, Marcucci G, Lee LJ, Delivery of antisense oligodeoxyribonucleotide lipopolyplex nanoparticles assembled by microfluidic hydrodynamic focusing. *J Control Release* 2010, 141 62–9, DOI: S0168–3659(09)00582–3 [pii] 10.1016/j.jconrel.2009.08.019. [PubMed: 19716852]
12. Bhaumik S, Walls Z, Puttaraju M, Mitchell LG, Gambhir SS, Molecular imaging of gene expression in living subjects by spliceosome-mediated RNA trans-splicing. *Proc Natl Acad Sci U S A* 2004, 101 8693–8, DOI: 10.1073/pnas.04027721010402772101 [pii]. [PubMed: 15161977]
13. Louie AY, Hüber MM, Ahrens ET, Rothbächer U, Moats R, Jacobs RE, Fraser SE, Meade TJ, In vivo visualization of gene expression using magnetic resonance imaging. *Nat. Biotechnol* 2000, 18 321–325. [PubMed: 10700150]
14. Weissleder R, Moore A, Mahmood U, Bhorade R, Benveniste H, Chiocca EA, Basilion JP, In vivo magnetic resonance imaging of transgene expression. *Nat Med* 2000, 6 351–5, DOI: 10.1038/73219. [PubMed: 10700241]
15. Rasaneh S, Rajabi H, Babaei MH, Akhlaghpour S, MRI contrast agent for molecular imaging of the HER2/neu receptor using targeted magnetic nanoparticles. *Journal of Nanoparticle Research* 2011, 13 2285–2293.
16. Zhang Y, Sun Y, Xu X, Zhang X, Zhu H, Huang L, Qi Y, Shen Y, Synthesis Biodistribution and Microsingle Photon Emission Computed Tomography (SPECT) Imaging Study of Technitium-99m Labeled PEGylated Dendrimer Poly(amidoamine) (PAMAM)-Folic Acid Conjugates. *J. Med. Chem* 2010, 53 3262–3272. [PubMed: 20350006]
17. Reichert JM, Valge-Archer VE, Development trends for monoclonal antibody cancer therapeutics. *Nat Rev Drug Discov* 2007, 6 349–56, DOI: nrd2241 [pii]10.1038/nrd2241. [PubMed: 17431406]
18. Kelly KA, Bardeesy N, Anbazhagan R, Gurumurthy S, Berger J, Alencar H, Depinho RA, Mahmood U, Weissleder R, Targeted nanoparticles for imaging incipient pancreatic ductal adenocarcinoma. *PLoS Med* 2008, 5 e85, DOI: 07-PLME-RA-1015 [pii]10.1371/journal.pmed.0050085. [PubMed: 18416599]
19. Bausch D, Thomas S, Mino-Kenudson M, Fernandez-del CC, Bauer TW, Williams M, Warshaw AL, Thayer SP, Kelly KA, Plectin-1 as a novel biomarker for pancreatic cancer. *Clin Cancer Res* 2011, 17 302–9, DOI: 1078–0432.CCR-10–0999 [pii]10.1158/1078-0432.CCR-10-0999. [PubMed: 21098698]
20. Zhao M, Beauregard DA, Loizou L, Davletov B, Brindle KM, Non-invasive detection of apoptosis using magnetic resonance imaging and a targeted contrast agent. *Nat Med* 2001, 7 1241–4, DOI: 10.1038/nm1101-1241nm1101-1241 [pii]. [PubMed: 11689890]
21. Jung HI, Kettunen MI, Davletov B, Brindle KM, Detection of apoptosis using the C2A domain of synaptotagmin I. *Bioconjug Chem* 2004, 15 983–7, DOI: 10.1021/bc049899q. [PubMed: 15366950]
22. Tsourkas A, Josephson L, in *Molecular Imaging Principles and Practice*, ed. Weissleder R, Ross BD, Rehemtulla A, Gambhir SS. People's Medical Publishing House-USA: Shelton, CT, 2010, pp 523–541.

23. Jain RK, Duda DG, Willett CG, Sahani DV, Zhu AX, Loeffler JS, Batchelor TT, Sorensen AG, Biomarkers of response and resistance to antiangiogenic therapy. *Nat Rev Clin Oncol* 2009, 6 327–38, DOI: nrclinonc.2009.63 [pii]10.1038/nrclinonc.2009.63. [PubMed: 19483739]
24. Heemels MT, Nature Insight Apoptosis. *Nature* 2000, 407 769.
25. Sa G, Das T, Anti cancer effects of curcumin: cycle of life and death. *Cell Division* 2008, 3 14. [PubMed: 18834508]
26. Hanahan D, Weinberg RA, Hallmarks of Cancer: The Next Generation. *Cell* 2011, 144 646–674. [PubMed: 21376230]
27. Sheikth-Hamad D, Timmins K, Jalali Z, Cisplatin-Induced Renal Toxicity: Possible Reversal by N-Acetylcysteine Treatment. *J. Am. Soc. Nephrol* 1997, 8 1640–1645. [PubMed: 9335396]
28. Li X, Li R, Qian X, Ding Y, Tu Y, Guo R, Hu Y, Jiang X, Guo W, Liu B, Superior antitumor efficiency of cisplatin-loaded nanoparticles by intratumoral delivery with decreased tumor metabolism rate. *Eur. J. Pharm. Biopharm* 2008, 70 726–734. [PubMed: 18634874]
29. Alexis F, Pridgen EM, Langer R, Farokhzad OC, Nanoparticle Technologies for Cancer Therapy. *Handb. Exp. Pharmacol* 2010, 197 55–86.
30. Vostrejs M, Moran PL, Seligman PA, Transferrin Synthesis by Small Cell Lung Cancer Cells Acts as an Autocrine Regulator of Cellular Proliferation. *J. Clin. Invest* 1988, 82 331–339. [PubMed: 2839550]
31. Neckers LM, Yenokida G, James SP, The Role of the Transferrin Receptor in Human B Lymphocyte Activation. *J. Immunol* 1984, 133 2437–2441. [PubMed: 6090534]
32. Chung MC, Structure and Function of Transferrin. *Biochem. Educ* 1984, 12 146–154.
33. Huang RK, Steinmetz NF, Fu C, Manchester M, Johnson JE, Transferrin-mediated targeting of bacteriophage HK97 nanoparticles into tumor cells. *Nanomedicine (Lond)* 2011, 6 55–68. [PubMed: 21182418]
34. Rae C, Koudelka KJ, Destito G, Estrada MN, Gonzalez MJ, Manchester M, Chemical Addressability of Ultraviolet-Inactivated Viral Nanoparticles (VNPs). *PLoS One* 2008, 30 e3315.
35. Liepold L, Anderson S, Willits D, Oltrogge L, Frank JA, Douglas T, Young M, Viral Capsids as MRI Contrast Agents. *Magn. Reson. Med* 2007, 58 871–879. [PubMed: 17969126]
36. Yildiz I, Shukla S, Steinmetz NF, Applications of viral nanoparticles in medicine *Curr. Opin. Biotech* 2011, 22 901–908. [PubMed: 21592772]
37. Grimm J, Perez JM, Josephson L, Weissleder R, Novel Nanosensors for Rapid Analysis of Telomerase Activity. *Cancer Res* 2004, 64 639–643. [PubMed: 14744779]
38. Antony AC, Folate Receptors. *Annu. Rev. Nutr* 1996, 16 501–521. [PubMed: 8839936]
39. Banerjee D, Harfouche R, Sengupta S, Nanotechnology-mediated targeting of tumor angiogenesis. *Vascular Cell* 2011, 3 3. [PubMed: 21349160]
40. Jain RK, Normalization of tumor vasculature: an emerging concept in antiangiogenic therapy. *Science* 2005, 307 58–62, DOI: 307/5706/58 [pii]10.1126/science.1104819. [PubMed: 15637262]
41. Zetter BR, Angiogenesis and tumor metastasis. *Annu Rev Med* 1998, 49 407–24, DOI: 10.1146/annurev.med.49.1.407. [PubMed: 9509272]
42. Brannon-Peppas L, Blanchette JO, Nanoparticle and targeted systems for cancer therapy. *Adv Drug Deliv Rev* 2004, 56 1649–59, DOI: 10.1016/j.addr.2004.02.014S0169409X04001450 [pii]. [PubMed: 15350294]
43. Maeda H, Wu J, Sawa T, Matsumura Y, Hori K, Tumor vascular permeability and the EPR effect in macromolecular therapeutics: a review. *J Control Release* 2000, 65 271–84, DOI: S0168–3659(99)00248–5 [pii]. [PubMed: 10699287]
44. Anderson SA, Rader RK, Westlin WF, Null C, Jackson D, Lanza GM, Wickline SA, Kotyk JJ, Magnetic resonance contrast enhancement of neovasculature with alpha(v)beta(3)-targeted nanoparticles. *Magn Reson Med* 2000, 44 433–9, DOI: 10.1002/1522-2594(200009)44:3<433::AID-MRM14>3.0.CO;2-9 [pii]. [PubMed: 10975896]
45. Ruoslahti E, RGD and other recognition sequences for integrins. *Annu Rev Cell Dev Biol* 1996, 12 697–715, DOI: 10.1146/annurev.cellbio.12.1.697. [PubMed: 8970741]

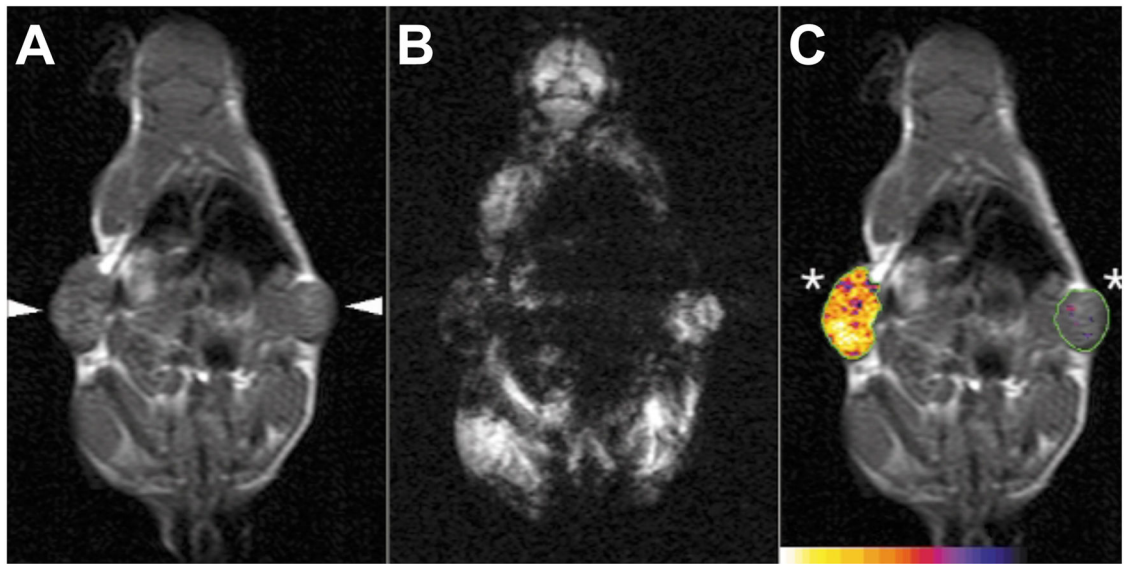
46. Ganta S, Devalapally H, Shahiwala A, Amiji M, A review of stimuli-responsive nanocarriers for drug and gene delivery. *J Control Release* 2008, 126 187–204, DOI: S0168–3659(08)00025–4 [pii]10.1016/j.jconrel.2007.12.017. [PubMed: 18261822]
47. Zhang C, Jugold M, Woenne EC, Lammers T, Morgenstern B, Mueller MM, Zentgraf H, Bock M, Eisenhut M, Semmler W, Kiessling F, Specific targeting of tumor angiogenesis by RGD-conjugated ultrasmall superparamagnetic iron oxide particles using a clinical 1.5-T magnetic resonance scanner. *Cancer Res* 2007, 67 1555–62, DOI: 67/4/1555 [pii]10.1158/0008-5472.CAN-06-1668. [PubMed: 17308094]
48. Liu S, Widom J, Kemp CW, Crews CM, Clardy J, Structure of human methionine aminopeptidase-2 complexed with fumagillin. *Science* 1998, 282 1324–7. [PubMed: 9812898]
49. Winter PM, Schmieder AH, Caruthers SD, Keene JL, Zhang H, Wickline SA, Lanza GM, Minute dosages of alpha(nu)beta3-targeted fumagillin nanoparticles impair Vx-2 tumor angiogenesis and development in rabbits. *FASEB J* 2008, 22 2758–67, DOI: fj.07–103929 [pii]10.1096/fj.07-103929. [PubMed: 18362202]
50. Kluz E, Jacobs I, Hectors SJ, Mayo KH, Griffioen AW, Strijkers GJ, Nicolay K, Dual-targeting of alpha(v)beta(3) and galectin-1 improves the specificity of paramagnetic/fluorescent liposomes to tumor endothelium in vivo. *J Control Release* 2011. DOI: S0168–3659(11)01004–2 [pii]10.1016/j.jconrel.2011.10.032.
51. Petrova TV, Makinen T, Alitalo K, Signaling via vascular endothelial growth factor receptors. *Exp Cell Res* 1999, 253 117–30, DOI: 10.1006/excr.1999.4707S0014-4827(99)94707-9 [pii]. [PubMed: 10579917]
52. Nugent MA, Iozzo RV, Fibroblast growth factor-2. *Int J Biochem Cell Biol* 2000, 32 115–20, DOI: S1357–2725(99)00123–5 [pii]. [PubMed: 10687947]
53. Davis S, Aldrich TH, Jones PF, Acheson A, Compton DL, Jain V, Ryan TE, Bruno J, Radziejewski C, Maisonpierre PC, Yancopoulos GD, Isolation of angiopoietin-1, a ligand for the TIE2 receptor, by secretion-trap expression cloning. *Cell* 1996, 87 1161–9, DOI: S0092–8674(00)81812–7 [pii]. [PubMed: 8980223]
54. Backer MV, Gaynutdinov TI, Patel V, Bandyopadhyaya AK, Thirumamagal BT, Tjarks W, Barth RF, Claffey K, Backer JM, Vascular endothelial growth factor selectively targets boronated dendrimers to tumor vasculature. *Mol Cancer Ther* 2005, 4 1423–9, DOI: 4/9/1423 [pii]10.1158/1535-7163.MCT-05-0161. [PubMed: 16170035]
55. Bermejo JF, Ortega P, Chonco L, Eritja R, Samaniego R, Mullner M, de Jesus E, de la Mata FJ, Flores JC, Gomez R, Munoz-Fernandez A, Water-soluble carbosilane dendrimers: synthesis biocompatibility and complexation with oligonucleotides; evaluation for medical applications. *Chemistry* 2007, 13 483–95, DOI: 10.1002/chem.200600594. [PubMed: 17004291]
56. Reichardt W, Hu-Lowe D, Torres D, Weissleder R, Bogdanov A Jr., Imaging of VEGF receptor kinase inhibitor-induced antiangiogenic effects in drug-resistant human adenocarcinoma model. *Neoplasia* 2005, 7 847–53. [PubMed: 16229807]
57. Reddy GR, Bhojani MS, McConville P, Moody J, Moffat BA, Hall DE, Kim G, Koo YE, Woolliscroft MJ, Sugai JV, Johnson TD, Philbert MA, Kopelman R, Rehemtulla A, Ross BD, Vascular targeted nanoparticles for imaging and treatment of brain tumors. *Clin Cancer Res* 2006, 12 6677–86, DOI: 12/22/6677 [pii]10.1158/1078-0432.CCR-06-0946. [PubMed: 17121886]
58. Schroeder A, Heller DA, Winslow MM, Dahlman JE, Pratt GW, Langer R, Jacks T, Anderson DG, Treating metastatic cancer with nanotechnology. *Nat Rev Cancer* 2012, 12 39–50, DOI: 10.1038/nrc3180nrc3180 [pii].
59. Goggins M, Identifying molecular markers for the early detection of pancreatic neoplasia. *Semin Oncol* 2007, 34 303–10, DOI: S0093–7754(07)00098-X [pii]10.1053/j.seminoncol.2007.05.003. [PubMed: 17674958]
60. Steeg PS, Tumor metastasis: mechanistic insights and clinical challenges. *Nat Med* 2006, 12 895–904, DOI: nm1469 [pii]10.1038/nm1469. [PubMed: 16892035]
61. Praetorius NP, Mandal TK, Engineered nanoparticles in cancer therapy. *Recent Pat Drug Deliv Formul* 2007, 1 37–51. [PubMed: 19075873]



62. Choi HS, Liu W, Misra P, Tanaka E, Zimmer JP, Itty Ipe B, Bawendi MG, Frangioni JV, Renal clearance of quantum dots. *Nat Biotechnol* 2007, 25 1165–70, DOI: nbt1340 [pii]10.1038/nbt1340. [PubMed: 17891134]
63. Li SD, Huang L, Pharmacokinetics and biodistribution of nanoparticles. *Mol Pharm* 2008, 5 496–504, DOI: 10.1021/mp800049w. [PubMed: 18611037]
64. Torabi M, Aquino SL, Harisinghani MG, Current concepts in lymph node imaging. *J Nucl Med* 2004, 45 1509–18, DOI: 45/9/1509 [pii]. [PubMed: 15347718]
65. Saokar A, Braschi M, Harisinghani M, Lymphotropic nanoparticle enhanced MR imaging (LNMRI) for lymph node imaging. *Abdom Imaging* 2006, 31 660–7, DOI: 10.1007/s00261-006-9006-2. [PubMed: 16680506]
66. Anzai Y, McLachlan S, Morris M, Saxton R, Lufkin RB, Dextran-coated superparamagnetic iron oxide, an MR contrast agent for assessing lymph nodes in the head and neck. *AJNR Am J Neuroradiol* 1994, 15 87–94. [PubMed: 7511324]
67. Anzai Y, Piccoli CW, Outwater EK, Stanford W, Bluemke DA, Nurenberg P, Saini S, Maravilla KR, Feldman DE, Schmiedl UP, Brunberg JA, Francis IR, Harms SE, Som PM, Tempny CM, Evaluation of neck and body metastases to nodes with ferumoxtran 10-enhanced MR imaging: phase III safety and efficacy study. *Radiology* 2003, 228 777–88, DOI: 10.1148/radiol.2283020872228/3/777 [pii]. [PubMed: 12954896]
68. Deserno WM, Harisinghani MG, Taupitz M, Jager GJ, Witjes JA, Mulders PF, van de Kaa Hulsbergen CA, Kaufmann D, Barentsz JO, Urinary bladder cancer: preoperative nodal staging with ferumoxtran-10-enhanced MR imaging. *Radiology* 2004, 233 449–56, DOI: 10.1148/radiol.23320311112332031111 [pii]. [PubMed: 15375228]
69. Ross RW, Zietman AL, Xie W, Coen JJ, Dahl DM, Shipley WU, Kaufman DS, Islam T, Guimaraes AR, Weissleder R, Harisinghani M, Lymphotropic nanoparticle-enhanced magnetic resonance imaging (LNMRI) identifies occult lymph node metastases in prostate cancer patients prior to salvage radiation therapy. *Clin Imaging* 2009, 33 301–5, DOI: S0899-7071(09)00024-2 [pii]10.1016/j.clinimag.2009.01.013. [PubMed: 19559353]
70. Stadnik TW, Everaert H, Makkat S, Sacre R, Lamote J, Bourgain C, Breast imaging. Preoperative breast cancer staging: comparison of USPIO-enhanced MR imaging and 18F-fluorodeoxyglucose (FDC) positron emission tomography (PET) imaging for axillary lymph node staging—initial findings. *Eur Radiol* 2006, 16 2153–60, DOI: 10.1007/s00330-006-0276-4. [PubMed: 16670863]
71. (a) Wang J, Chen C, Li B, Yu H, Zhao Y, Sun J, Li Y, Xing G, Yuan H, Tang J, Chen Z, Meng H, Gao Y, Ye C, Chai Z, Zhu C, Ma B, Fang X, Wan L, Antioxidative function and biodistribution of [Gd@C82(OH)22]n nanoparticles in tumor-bearing mice. *Biochem Pharmacol* 2006, 71 872–81, DOI: S0006-2952(05)00795-1 [pii]10.1016/j.bcp.2005.12.001; [PubMed: 16436273] (b) Nguyen HL, Zucker S, Zarrabi K, Kadam P, Schmidt C, Cao J, Oxidative stress and prostate cancer progression are elicited by membrane-type 1 matrix metalloproteinase. *Mol Cancer Res* 2011, 9 1305–18, DOI: 1541-7786.MCR-11-0033 [pii]10.1158/1541-7786.MCR-11-0033. [PubMed: 21849471]
72. Meng H, Xing G, Blanco E, Song Y, Zhao L, Sun B, Li X, Wang PC, Korotcov A, Li W, Liang X, Chen C, Yuan H, Zhao F, Chen Z, Sun T, Chai Z, Ferrari M, Zhao Y, Gadolinium metallofullerenol nanoparticles inhibit cancer metastasis through matrix metalloproteinase inhibition: imprisoning instead of poisoning cancer cells. *Nanomedicine* 2012, 8 136–146. [PubMed: 21930111]
73. Olson ES, Jiang T, Aguilera TA, Nguyen QT, Ellies LG, Scadeng M, Tsien RY, Activatable cell penetrating peptides linked to nanoparticles as dual probes for in vivo fluorescence and MR imaging of proteases. *Proc. Natl. Acad. Sci. U. S. A.* 2010, 107 4311–4316. [PubMed: 20160077]
74. Penet MF, Glunde K, Jacobs MA, Pathak AP, Bhujwala ZM, Molecular and functional MRI of the tumor microenvironment. *J Nucl Med* 2008, 49 687–90, DOI: jnumed.107.043349 [pii]10.2967/jnumed.107.043349. [PubMed: 18413382]
75. Del Vecchio S, Zannetti A, Iommelli F, Lettieri A, Brunetti A, Salvatore M, Molecular imaging of tumor microenvironment: challenges and perspectives. *Q J Nucl Med Mol Imaging* 2010, 54 249–58, DOI: R39102264 [pii]. [PubMed: 20639812]
76. Jain RK, Transport of molecules, particles, and cells in solid tumors. *Annu Rev Biomed Eng* 1999, 1 241–63, DOI: 1/1/241 [pii]10.1146/annurev.bioeng.1.1.241. [PubMed: 11701489]

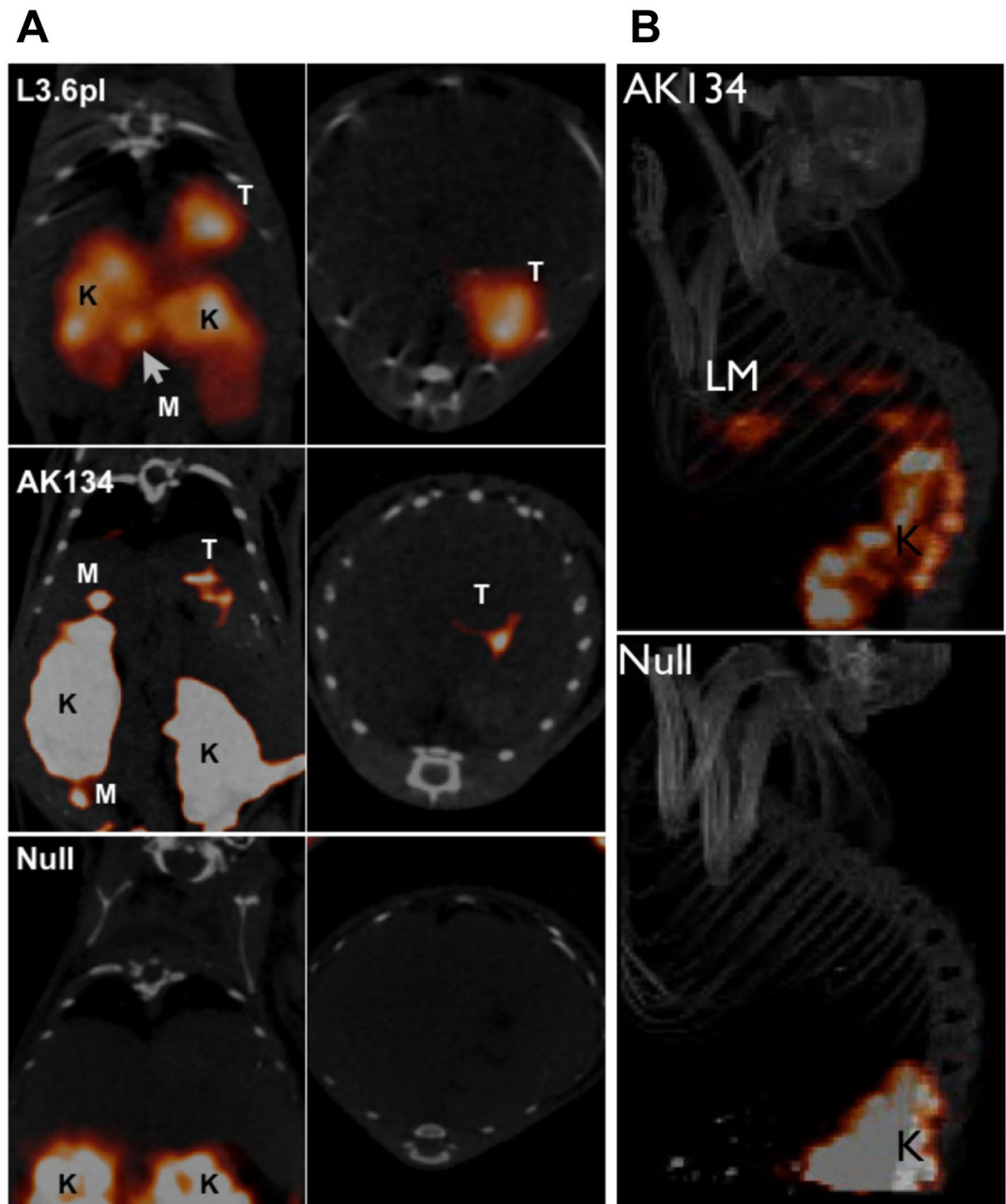
77. Lochter A, Bissell MJ, Involvement of extracellular matrix constituents in breast cancer. *Semin Cancer Biol* 1995, 6 165–73, DOI: 10.1006/scbi.1995.0017S1044-579X(85)70017-X [pii]. [PubMed: 7495985]
78. Liotta LA, Rao CN, Role of the extracellular matrix in cancer. *Ann N Y Acad Sci* 1985, 460 333–44. [PubMed: 3008626]
79. Lane TF, Sage EH, The biology of SPARC, a protein that modulates cell-matrix interactions. *FASEB J* 1994, 8 163–73. [PubMed: 8119487]
80. Sage EH, Bornstein P, Extracellular proteins that modulate cell-matrix interactions. SPARC, tenascin, and thrombospondin. *J Biol Chem* 1991, 266 14831–4. [PubMed: 1714444]
81. Tremble PM, Lane TF, Sage EH, Werb Z, SPARC, a secreted protein associated with morphogenesis and tissue remodeling, induces expression of metalloproteinases in fibroblasts through a novel extracellular matrix-dependent pathway. *J Cell Biol* 1993, 121 1433–44. [PubMed: 8509459]
82. Clark CJ, Sage EH, A prototypic matricellular protein in the tumor microenvironment--where there's SPARC, there's fire. *J Cell Biochem* 2008, 104 721–32, DOI: 10.1002/jcb.21688. [PubMed: 18253934]
83. Thomas S, Waterman P, Chen S, Marinelli B, Seaman M, Rodig S, Ross RW, Josephson L, Weissleder R, Kelly KA, Development of Secreted Protein and Acidic and Rich in Cysteine (SPARC) Targeted Nanoparticles for the Prognostic Molecular Imaging of Metastatic Prostate Cancer. *J Nanomed Nanotechnol* 2011, 2 DOI: 2157–7439-2–112 [pii]10.4172/2157-7439.1000112.
84. Kelly KA, Allport JR, Yu AM, Sinh S, Sage EH, Gerszten RE, Weissleder R, SPARC is a VCAM-1 counter-ligand that mediates leukocyte transmigration. *J Leukoc Biol* 2007, 81 748–56, DOI: jlb.1105664 [pii]10.1189/jlb.1105664. [PubMed: 17178915]
85. Condeelis J, Pollard JW, Macrophages: obligate partners for tumor cell migration, invasion, and metastasis. *Cell* 2006, 124 263–6, DOI: S0092–8674(06)00055–9 [pii]10.1016/j.cell.2006.01.007. [PubMed: 16439202]
86. Pollard JW, Tumour-educated macrophages promote tumour progression and metastasis. *Nat Rev Cancer* 2004, 4 71–8, DOI: 10.1038/nrc1256nrc1256 [pii]. [PubMed: 14708027]
87. Bingle L, Brown NJ, Lewis CE, The role of tumour-associated macrophages in tumour progression: implications for new anticancer therapies. *J Pathol* 2002, 196 254–65, DOI: 10.1002/path.1027 [pii]10.1002/path.1027. [PubMed: 11857487]
88. Nagaraj S, Gupta K, Pisarev V, Kinarsky L, Sherman S, Kang L, Herber DL, Schneck J, Gabrilovich DI, Altered recognition of antigen is a mechanism of CD8+ T cell tolerance in cancer. *Nat Med* 2007, 13 828–35, DOI: nm1609 [pii]10.1038/nm1609. [PubMed: 17603493]
89. Daldrup-Link HE, Golovko D, Ruffell B, Denardo DG, Castaneda R, Ansari C, Rao J, Tikhomirov GA, Wendland MF, Corot C, Coussens LM, MRI of tumor-associated macrophages with clinically applicable iron oxide nanoparticles. *Clin Cancer Res* 2011, 17 5695–704, DOI: 1078–0432.CCR-10–3420 [pii]10.1158/1078-0432.CCR-10-3420. [PubMed: 21791632]
90. Vaupel P, Physiological properties of malignant tumours. *NMR Biomed* 1992, 5 220–5. [PubMed: 1449960]
91. Prescott DM, Charles HC, Poulson JM, Page RL, Thrall DE, Vujaskovic Z, Dewhirst MW, The relationship between intracellular and extracellular pH in spontaneous canine tumors. *Clin Cancer Res* 2000, 6 2501–5. [PubMed: 10873105]
92. Bae Y, Jang WD, Nishiyama N, Fukushima S, Kataoka K, Multifunctional polymeric micelles with folate-mediated cancer cell targeting and pH-triggered drug releasing properties for active intracellular drug delivery. *Mol Biosyst* 2005, 1 242–50, DOI: 10.1039/b500266d. [PubMed: 16880988]
93. Lim EK, Huh YM, Yang J, Lee K, Suh JS, Haam S, pH-triggered drug-releasing magnetic nanoparticles for cancer therapy guided by molecular imaging by MRI. *Adv Mater* 2011, 23 2436–42, DOI: 10.1002/adma.201100351. [PubMed: 21491515]
94. Krohn KA, Link JM, Mason RP, Molecular imaging of hypoxia. *J Nucl Med* 2008, 49 Suppl 2 129S–48S, DOI: 49/Suppl\_2/129S [pii]10.2967/jnumed.107.045914. [PubMed: 18523070]

95. Hockel M, Vaupel P, Tumor hypoxia: definitions and current clinical, biologic, and molecular aspects. *J Natl Cancer Inst* 2001, 93 266–76. [PubMed: 11181773]
96. Melo T, Duncan J, Ballinger JR, Rauth AM, BRU59–21, a second-generation <sup>99m</sup>Tc-labeled 2-nitroimidazole for imaging hypoxia in tumors. *J Nucl Med* 2000, 41 169–76. [PubMed: 10647620]
97. Glunde K, Gillies RJ, Neeman M, Bhujwala ZM, in *Molecular Imaging*, ed. Weissleder R, Ross BD, Rehemtulla A, Gambhir SS. People's Medical Publishing House-USA: Shelton, CT, 2010, vol. s, pp 844–863.
98. Napp J, Behnke T, Fischer L, Wurth C, Wottawa M, Katschinski DM, Alves F, Resch-Genger U, Schaferling M, Targeted luminescent near-infrared polymer-nanoprobes for in vivo imaging of tumor hypoxia. *Anal Chem* 2011, 83 9039–46, DOI: 10.1021/ac201870b. [PubMed: 22007722]



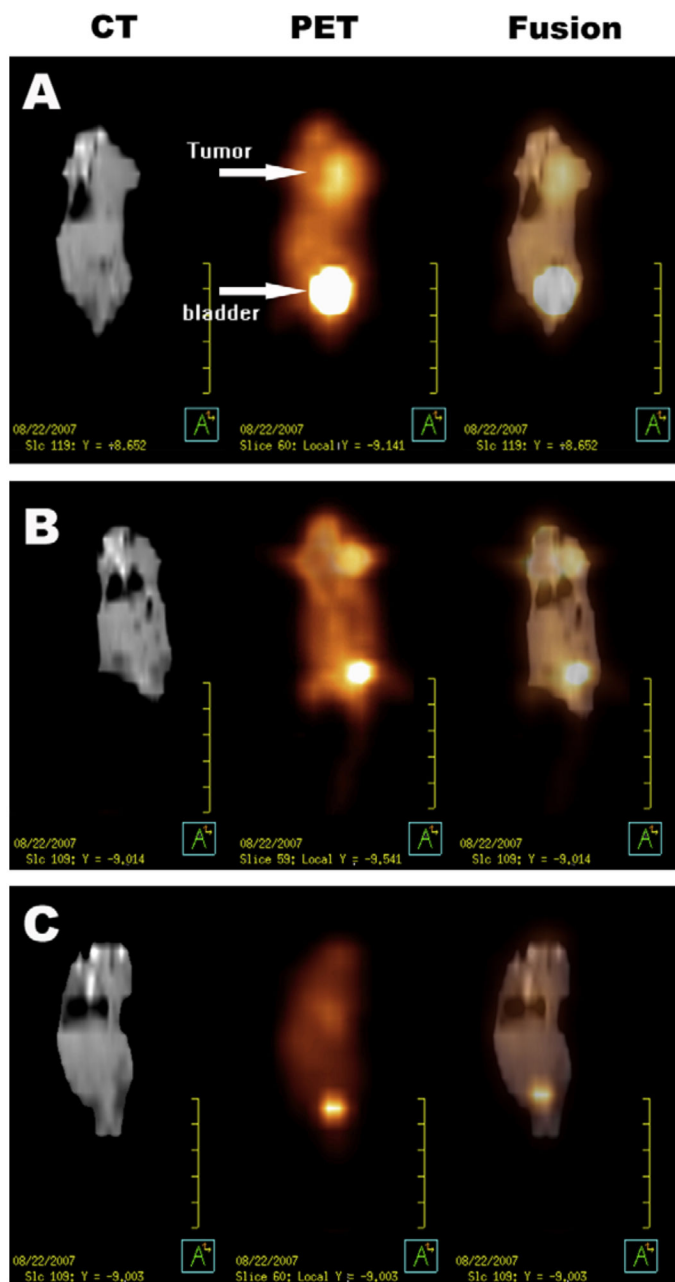
**Figure 1. *In vivo* MRI of engineered transferrin receptor (ETR)+ (left arrowhead) and ETR- (right arrowhead) flank tumors.**

**A)** T1-weighted coronal spin echo image showing similar signal intensities between ETR+ and ETR- tumor. **B)** T2-weighted gradient-echo image showing a substantial differences between ETR+ and ETR- tumors. ETR-mediated cellular accumulation of superparamagnetic probe decreases signal intensity. **C)** Composite image of a T1-weighted spin-echo image detailed with R2 changes after Tf-MION administration. Reproduced from Weissleder *et al.*<sup>14</sup>



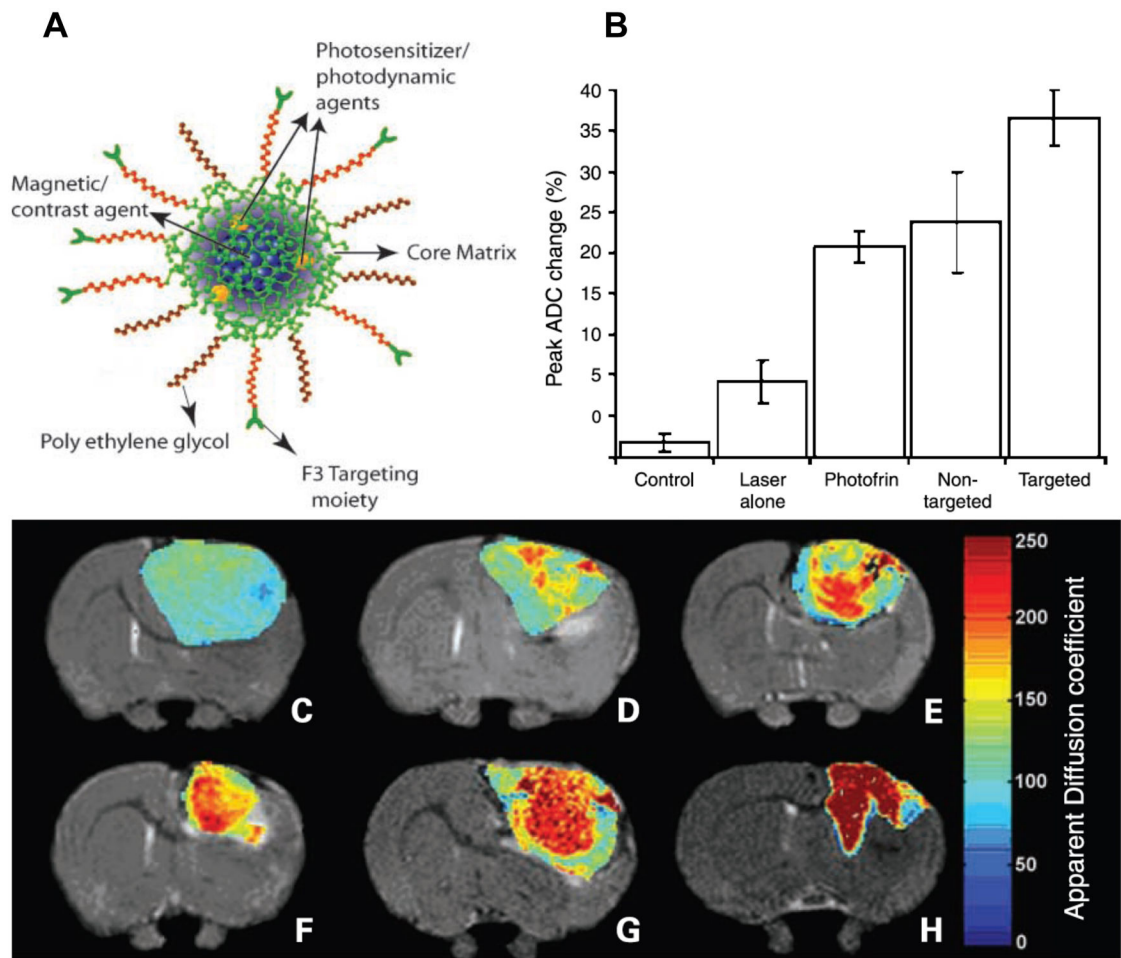
**Figure 2.**

In vivo imaging of plectin in orthotopic pancreatic cancer and liver metastases. A) Mice bearing tumors from orthotopically implanted L3.6pl, AK134 cells, and saline (null) were injected with  $^{111}\text{In}$ -tPTP. Imaging via SPECT/CT 4 hours post injection shows that tPTP accumulated in PDAC. Coronal (left) and axial (right) SPECT/CT slices through the tumor. T, tumor; K, kidney; M, peritoneal metastasis. B) AK134 cells, or saline (null), were injected intrasplenically to produce liver metastases. Top, mice with liver metastasis (LM) from AK134 injection. Bottom, null animals without tumor cell injected. K, kidney. Adapted from Bausch et al.<sup>19</sup>



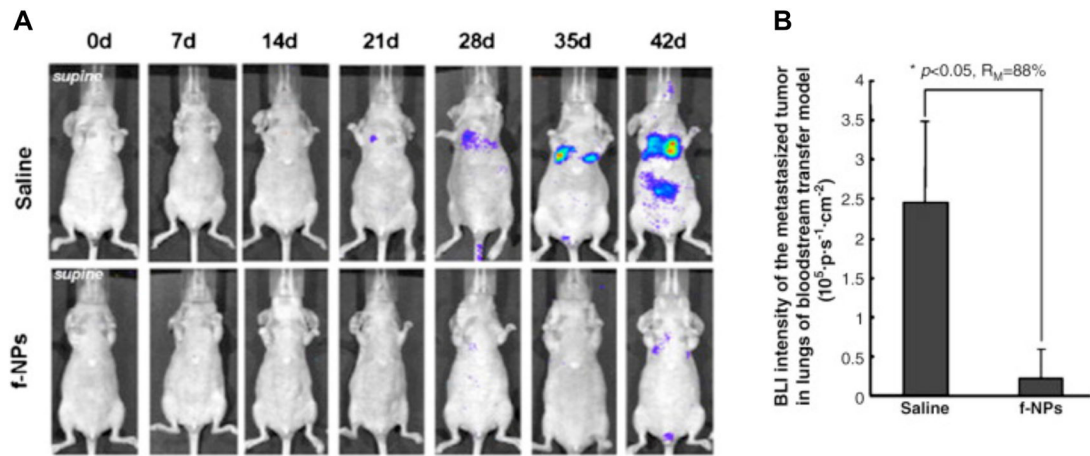
**Figure 3. Male ICR mice bearing a subcutaneous H22 (murine hepatoma cell line) tumor at the left side of the thorax.**

**A)** Coronal images of a mouse in the control group (saline). **B)** Coronal images of a mouse in the group receiving intratumoral free cisplatin (5 mg/kg). **C)** Coronal images of a mouse in the group receiving intratumoral cisplatin-loaded nanoparticles (5 mg/kg). Reproduced from Li *et al.*<sup>28</sup>



**Figure 4. Vascular targeted photodynamic therapy (PDT) with theranostic agents.**

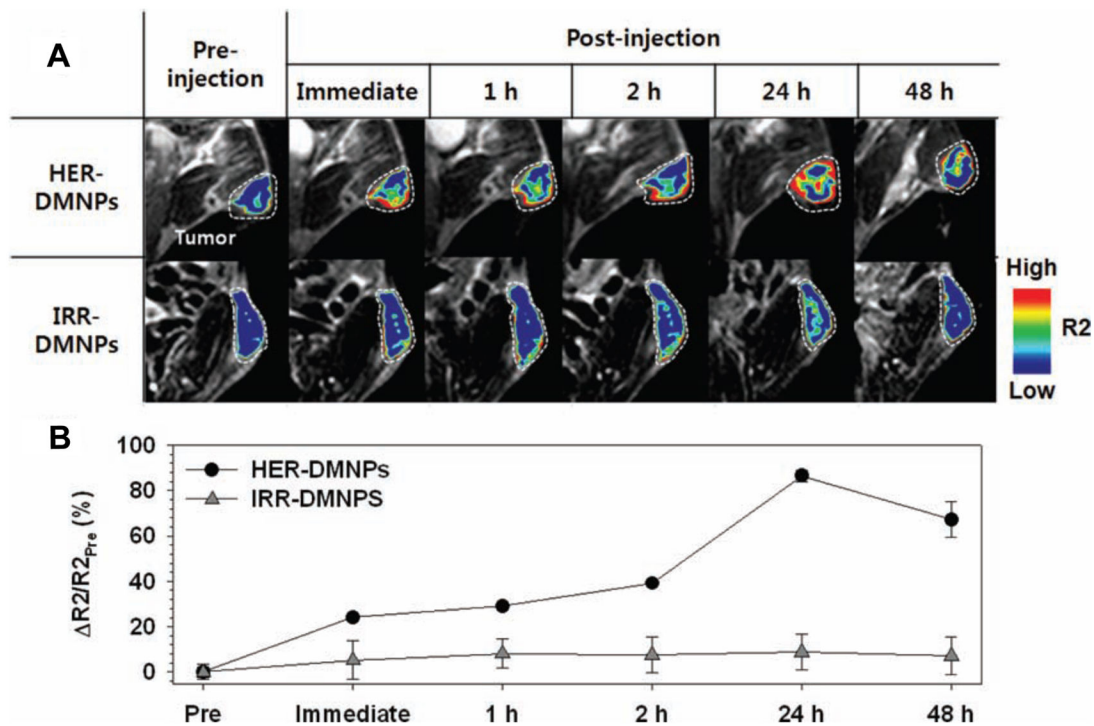
**A)** Schematic representation of the multifunctional nanoparticles. The core of the nanoparticle was synthesized from polyacrylamide, which was embedded with PDT dyes (Photofrin) and/or imaging agents (magnetite/fluorochrome). Polyethylene glycol linker and a molecular address tag (F3 peptide) were attached to target these nanoparticles to cancer cells. **B)** Mean peak percentage change in tumor apparent diffusion coefficient values for each of the experimental groups; bars, SE. **C)** T2-weighted MRI at day 8 after treatment from a representative control i.c. 9L tumor and **D)** tumors treated with laser light only, **E)** i.v. administration of Photofrin plus laser light, and **F)** nontargeted nanoparticles containing Photofrin plus laser light and **G)** targeted nanoparticles containing Photofrin plus laser light. The image shown in **H)** is from the same tumor shown in **G)**, which was treated with the F3-targeted nanoparticle preparation but at day 40 after treatment. The color diffusion maps overlaid on top of T2-weighted images represent the apparent diffusion coefficient (ADC) distribution in each tumor slice shown. Adapted from Reddy *et al.*<sup>57</sup>



**Figure 5. MMP-targeting f-NPs inhibit the tumorigenesis in the blood transfer model of MDA-MB-231-luc cancer mice.**

**A)**  $1 \times 10^6$  MDA-MB-231-luc cells were injected into the tail vein of the nude mice. Seven days after injection, the mice received daily intraperitoneal doses of the f-NPs at  $2.5 \mu\text{mol/kg}$  for a duration of 6 weeks. Saline was used as control. Tumor metastases in lung were monitored weekly by bioluminescence imaging (BLI). **B)** Quantification of the BLI intensity of tumor foci in the lungs of animals after different treatments. f-NPs treatment significantly inhibited tumor metastasis. \* $P < 0.05$ , compared to control. Reproduced from Meng *et al.*<sup>72</sup>



**Figure 6.**

A) Color-coded T2-weighted MR images of tumor-bearing mice after the intravenous injection of HER2/neu antibody (herceptin)-modified pH-sensitive drug-delivering magnetic nanoparticles (HER-DMNPs) and DMNPs modified with an irrelevant antibody (IRR-DMNPs) at various time intervals, respectively. Tumor regions are indicated with a white dashed boundary. B)  $R2/R2_{Pre}$  graph versus time after the injection of HER-DMNPs (black circle) and IRR-DMNPs (gray triangle). Reproduced from Lim *et al*<sup>93</sup>

Table 1.

Summary of nanoparticle technologies discussed in the text

Discerning Cancer Characteristics	Targets	Nanoparticles	Imaging Modality	Application	Nanoparticle Status	Ref.
Genetic mutations	Mutated or overexpressed gene	Fluorophore-conjugated molecular beacon (MB) targeting survivin and cyclin D1 mRNA	Optical	Theragnostic	Preclinical ( <i>in vitro</i> )	2
		Magnetofluorescent nanoparticle conjugated with miRNA-221 MB and ASI411 aptamer	MRI, Optical	Theragnostic	Preclinical ( <i>in vivo</i> )	6
		Polyamidoamine dendrimer, conjugated with biotin and avidin with radiolabeled antisense oligonucleotide (RASON)	Scintigraphy	Theragnostic	Preclinical ( <i>in vivo</i> )	7
Protein misregulation	Overexpressed protein	Caged paramagnetic nanoparticle activated by $\beta$ -galactosidase reporter gene	MRI	Monitoring therapy	Preclinical ( <i>in vivo</i> )	13
		Dextran-coated MION conjugated with holo-transferrin	MRI	Monitoring therapy	Preclinical ( <i>in vivo</i> )	14
		Dextran-coated iron oxide nanoparticle conjugated with Trastuzumab	MRI	Theragnostic	Preclinical ( <i>in vivo</i> )	15
		$^{99m}\text{Tc}$ labeled PEGylated dendrimer with folic acid	SPECT	Diagnostic	Preclinical ( <i>in vivo</i> )	16
		$^{111}\text{In}$ -labeled tetrameric plectin-targeting peptide nanoparticle	SPECT, CT	Early detection	In development for clinical trial	19
Proliferation	Uncontrolled cell division	$\text{C}_2$ -Synaptotagmin I-conjugated SPION	MRI	Monitoring drug efficacy	Preclinical ( <i>in vivo</i> )	20
		Annexin-V-targeted CLION	MRI	Monitoring drug efficacy	Phase II clinical trial	22
		mPEG-PCl nanoparticle encapsulated with cisplatin in combination with $^{18}\text{F}$ -FDG	MRI, PET	Theragnostic	Preclinical ( <i>in vivo</i> )	28
		HK97-based viral nanoparticle conjugated with fluorescein-5-maleimide	Optical	Theragnostic	Preclinical ( <i>in vitro</i> )	33
Angiogenesis	Integrin $\alpha_v\beta_3$	CLIO-NH <sub>2</sub> nanoparticle conjugated with ITAGGG (telomerase synthesized)	MRI	Diagnostic	Preclinical ( <i>in vitro</i> )	37
		$^{99m}\text{Tc}$ labeled PEGylated dendrimer with folic acid	SPECT	Diagnostic	Preclinical ( <i>in vivo</i> )	16
		USPION coated with APTMS and conjugated with RGD peptides	MRI	Diagnostic	Preclinical ( <i>in vivo</i> )	46
		$\alpha_v\beta_3$ -targeted perfluorocarbon nanoparticle conjugated with fumagillin, modified with paramagnetic chelates	MRI, Optical	Theragnostic	Preclinical ( <i>in vivo</i> )	48
		Paramagnetic liposomal nanoparticle with RGD and angixen	MRI	Diagnostic	Preclinical ( <i>in vivo</i> )	49

Discerning Cancer Characteristics	Targets	Nanoparticles	Imaging Modality	Application	Nanoparticle Status	Ref.
	VEGF	Boronated dendrimers with VEGF <sub>121</sub>	Optical	Diagnostic	Preclinical ( <i>in vivo</i> )	53
	Nucleolin	T2-type MION with VEGF tyrosinase kinase inhibitors	MRI	Early detection	Preclinical ( <i>in vivo</i> )	55
		Vascular targeting nanoparticle conjugated with F3 peptide and photofrin	MRI	Theragnostic	Preclinical ( <i>in vivo</i> )	56
Invasion & metastasis	Lymph node metastasis	Ferumoxtran-10 (USPIO)	MRI	Early detection, Theragnostic	Phase III clinical trial	62-66
	MMP (ECM degradation)	Gadolinium metallofullerenol nanoparticles	MRI	Theragnostic	Preclinical ( <i>in vivo</i> )	68
		Dendritic nanoparticles conjugated with gadolinium-labeled activatable cell penetrating peptides (ACPPs)	MRI	Diagnostic	Preclinical ( <i>in vivo</i> )	69
Abnormal microenvironment	Low extracellular pH	Polymeric-micelle encapsulated with folate, Adriamycin, and hydrazone (for pH-dependent release)	NMR, Flow cytometry	Therapy	Preclinical ( <i>in vivo</i> )	88
		Iron oxide nanoparticles conjugated with HER2/neu antibody and doxorubicin coated with pH-sensitive polymer	MRI	Theragnostic	Preclinical ( <i>in vivo</i> )	89
	Hypoxia	Polystyrene nanoparticles with oxygen-sensitive palladium mesotetraphenylporphyrin and herceptin	Optical imaging	Diagnostic	Preclinical ( <i>in vivo</i> )	94
	Macrophage / leukocyte infiltration	Ferumoxtyol (Second-generation USPIO)	MRI	Diagnostic	Phase II clinical trial	85
		SPARC-targeted nanoparticle with an iron oxide core	Optical (FMT), CT	Diagnostic	Preclinical ( <i>in vivo</i> )	79